Optics Communications 333 (2014) 209–212

Contents lists available at ScienceDirect

Optics Communications

journal homepage: www.elsevier.com/locate/optcom

Reconfigurable microwave photonic filter based on tunable dispersion-induced power fading in a dispersive element

Wen Ting Wang, Wei Li*, Wen Hui Sun, JianGuo Liu, Hai Qing Yuan, Ning Hua Zhu

State Key Laboratory on Integrated Optoelectronics, Institute of Semiconductors, Chinese Academy of Sciences, Beijing 100083, China

ARTICLE INFO

Article history:
Received 12 April 2014
Received in revised form
26 June 2014
Accepted 30 July 2014
Available online 11 August 2014

Keywords:
Microwave photonic filter
Dispersion-induced power fading
Wide tenability
Reconfigurability

ABSTRACT

We propose and demonstrate a reconfigurable microwave photonic filter (MPF) based on tunable dispersion-induced power fading (DIPF) in a dispersive element. A multi-wavelength optical signal is used to generate the multi-taps of the MPF. A polarization modulator (PolM), a polarization controller (PC), and a polarizer are cascaded to build a new modulator which can be regarded as an intensity modulator, a phase modulator, or an intensity and phase hybrid modulator by adjusting the PC. A dispersive element is followed after the PC to generate the DIPF which is controllable by tuning the PC. In this way, the MPF is reconfigurable and tunable. The proposed method is theoretically analyzed and experimentally verified. The simulated results fit well with the experimental ones.

1. Introduction

Microwave photonic filters (MPFs) have attracted considerable attentions due to its widespread applications including a radio-over-fiber system, optically controlled phased-array antennas, and a radar system and its inherent advantages brought by photonic technologies, such as light weight, high bandwidth, low loss, wide tunability, reconfigurability, and insensitivity to electromagnetic interference [1–4]. Various methods have been proposed to design the MPFs, most of which are based on the incoherent operation to avoid the optical interference. However, only positive coefficient can be generated because the intensity is always positive [1–4]. The MPF with positive coefficient has a low-pass frequency response. In order to realize the band-pass microwave filters, negative coefficients are needed [5–10]. Up to now, various configurations of MPFs with negative coefficient have been realized based on π phase shift in an electro-optic modulator [5,6], cross polarization modulation or cross phase modulation in a highly nonlinear fiber (HNLF) [7,8]. Zeng et al. reported a MPF with equivalent negative coefficient based on phase-to-intensity modulation conversion in a dispersive element [11]. The frequency response of the MPF is determined by both the basic frequency responses of the multi-tap MPF and the DIPF induced by the dispersive element. This method is very promising since it is easy to be expanded to multi-tap MPF with band-pass response [12,13]. However, it suffers from the limitation that the DIPF is fixed for a given dispersive element. Thus, the MPF is not flexible and reconfigurable for practical applications. In fact, many efforts have been made to design highly reconfigurable MPFs. In Ref. [14], highly reconfigurable MPFs have been proposed based on non-sliced broadband optical source and arbitrarily user-defined Wave Shaper. Although the MPF is highly reconfigurable, the system is bulky and costly.

In this paper, we report a reconfigurable MPF based on a tunable DIPF in a dispersive element. Compared with Ref. [14], the system of the proposed MPF is simple and cost efficient. In our scheme, a multi-wavelength optical source is used to generate the multi-taps of the MPF with the basic transmission response. The cascaded polarization modulator (PolM), a polarization controller (PC), and a polarizer are equivalent to a new modulator which can be regarded as an intensity modulator, a phase modulator, or an intensity and phase hybrid modulator by adjusting the PC. A dispersive element is used to generate the DIPF which is controllable by tuning the PC. Therefore, the proposed MPF is reconfigurable by tuning the DIPF via the PC. The proposed MPF is theoretically analyzed and experimentally demonstrated. The simulated and the experimental results agree well with each other.

2. Operational principle

The schematic diagram of the proposed MPF is shown in Fig. 1. An optical carrier from a laser diode (LD) is sent to a Mach-Zehnder modulator (MZM) to generate a multi-wavelength optical signal which is equally spaced with a frequency interval corresponding to the frequency of the microwave source (MS). This optical signal is launched to a PolM which is followed by a PC and a polarizer. A dispersive element is used to generate the DIPF and

* Corresponding author.
E-mail address: liwei05@semi.ac.cn (W. Li).

http://dx.doi.org/10.1016/j.optcom.2014.07.089
0030-4018/

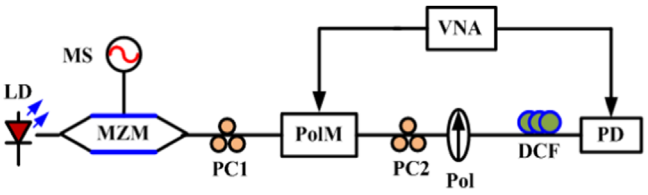

Fig. 1. Schematic diagram of the proposed MPF (LD: laser diode; MS: microwave source; MZM: Mach-Zehnder modulator; PC: polarization controller; PolM: polarization modulator; Pol: polarizer; PD: photodetector; DCF: dispersion compensation fiber; VNA: vector network analyzer.).

to introduce a basic time delay between the different taps of the MPF. A photodetector (PD) is used to convert the optical signal to the electrical signal. The frequency response of the MPF is measured by a vector network analyzer (VNA). First of all, we assume that only a single optical carrier is sent to the PolM which is a special phase modulator that supports modulation on both TE and TM modes with opposite phase modulation indices. Mathematically, the optical field at the output of the PolM can be expressed as

$$E_{PolM}(t)=\begin{bmatrix}E_x\\E_y\end{bmatrix}\propto\begin{bmatrix}\exp j(\omega_0 t+\beta\ \cos(\omega_m t))\\ \exp j(\omega_0 t-\beta\ \cos(\omega_m t))\end{bmatrix} \tag{1}$$

Where ω_0 is the angular frequency of the optical carrier, $\beta=\pi V_m/V_\pi$ is the phase modulation index of the PolM, V_π is the half-wave voltage of the PolM, ω_m and V_m are the angular frequency and amplitude of the sinusoidal microwave signal applied to the PolM, respectively. Applying Jacobi–Anger expansion to Eq. (1) and considering the small-signal modulation condition, we have

$$\vec{E}_{PolM}(t)=\begin{bmatrix}E_x\\E_y\end{bmatrix}\propto\exp(j\omega_0 t)\begin{bmatrix}J_0(\beta)+J_1(\beta)\exp j(\omega_m t+\pi/2)\\ +J_1(\beta)\exp j(-\omega_m t+\pi/2)\\ J_0(\beta)-J_1(\beta)\exp j(\omega_m t+\pi/2)\\ -J_1(\beta)\exp j(-\omega_m t+\pi/2)\end{bmatrix} \tag{2}$$

where $J_n(\cdot)$ is the nth-order Bessel function of the first kind. As can be seen from Eq. (2), the state of polarizations (SOPs) of the optical carrier and sidebands are oriented at 45° and −45° to E_x, respectively [15]. The PC2 is used to introduce a static phase difference φ between the two orthogonal SOPs. Thus, we have

$$\vec{E}_{Polm}(t)=\begin{bmatrix}E_{x+45^\circ}\\E_{y+45^\circ}\end{bmatrix}\propto\exp(j\omega_0 t)\begin{bmatrix}J_1(\beta)\exp j(\omega_m t+\pi/2)\\ +J_1(\beta)\exp j(-\omega_m t+\pi/2)\\ J_0(\beta)\exp j\varphi\end{bmatrix} \tag{3}$$

The Pol oriented at 45° to the SOP of the optical carrier is used to project the optical carrier and sidebands onto a fixed polarization state, the electrical field at the output of the Pol is given by

$$E_{Pol}\propto\frac{1}{\sqrt{2}}\exp(j\omega_0 t)[J_0(\beta)\exp(j\varphi)+J_1(\beta)\exp j(\omega_m t+\pi/2)+J_1(\beta)\exp j(-\omega_m t+\pi/2)] \tag{4}$$

The optical signal at the output of the Pol is sent to a dispersive element, which served as a phase filter. The transfer response of the dispersive element can be described as

$$\exp j\Phi(\omega)=\exp j[\ddot{\Phi}(\omega-\omega_0)^2/2] \tag{5}$$

where $\ddot{\Phi}$ is the first-order dispersion coefficient. The electrical field at the output of the dispersive element is given by

$$E_{Pol}\propto\exp(j\omega_0 t)\{J_0(\beta)\exp(j\varphi)+J_1(\beta)\exp(j\omega_m t+j\pi/2+j\omega_m^2\ddot{\Phi}/2)+J_1(\beta)\exp(-j\omega_m t+j\pi/2+j\omega_m^2\ddot{\Phi}/2)\} \tag{6}$$

After square-law detection by the PD, the microwave photocurrent of interest can be expressed as

$$i(t)\propto\ \sin\left(\frac{\ddot{\Phi}\omega_m^2}{2}-\varphi\right)\cos\ \omega_m t \tag{7}$$

As can be seen from Eq. (7), the microwave signal at the angular frequency of ω_m is detected. It is clearly seen that the amplitude is determined by a sine term, which is the well-known DIPF effect. However, it is worth noting that the DIPF is not fixed in our case, it is tunable by adjusting the phase difference φ (or the PC2) [16,17]. For a MPF with multi-taps, multi-wavelength optical signals are used. Applying Fourier transform to both sides of Eq. (7) and considering multi-taps, the frequency response of the MPF is given by

$$H(\omega_m)\propto\ \sin\left(\frac{\ddot{\Phi}\omega_m^2}{2}-\varphi\right)\sum_{n=1}^{N}P_n\exp[j\omega_m(n-1)T] \tag{8}$$

where N is the tap number of the MPF, T is the time delay between the adjacent taps which is introduced by the dispersive element. P_n is the tap-weight coefficients of the nth optical carrier. As can be seen from Eq. (8), the frequency response of the MPF consists of two parts. One is the tunable DIPF and the other is the basic frequency response of the multi-tap MPF. If $\varphi=0$, the frequency response of the proposed MPF has equivalent negative coefficients as reported in Refs. [11–13,18]. However, it suffers from the limitation that the DIPF is fixed for a given dispersive element. To realize a tunable MPF, the tap number can be adjusted as reported in Ref. [18]. However, different from the previous methods, the proposed MPF is reconfigurable by tuning the DIPF.

3. Experiment and simulation

An experiment based on the setup shown in Fig. 1 is carried out to demonstrate the proposed MPF. A linearly polarized optical carrier from a laser diode (LD) emitting at the wavelength of 1550 nm was fiber-coupled to a MZM with a bandwidth of 40 GHz. The MZM was driven by a microwave signal from a microwave source (MS). By properly adjusting the bias of the MZM, three-tap optical signal with equal frequency spacing and power was generated to serve as the multi-wavelength optical signal. A part of the optical power (20%) from the output of the MZM was extracted by an optical coupler and measured by an optical spectrum analyzer (OSA) with a resolution of 0.01 nm. The 80% part optical signal was sent to a PolM with a half-wave voltage of 3.5 V and a bandwidth of 40 GHz through a PC1. The PolM has an internal polarizer which is oriented at an angle of 45° to the principal axis of the PolM. The optical signal at the output of the polarizer was sent into a dispersion compensate fiber (DCF) which has a length of 1034 m and an accumulated dispersion of 447.5 ps/nm at 1550 nm. The optical signal at the output of the DCF was sent to a PD which has a bandwidth of 40 GHz. A 40 GHz VNA was used to measure the transmission frequency response of the MPF.

First of all, the frequency of the microwave signal driven to the MZM was chosen to be 17 GHz. The optical signal generated after the MZM is shown in Fig. 2(a). As can be seen, a three-line flat optical signal was generated with undesired sidebands suppression of 11 dB. The MPF was designed to generate a high-pass transmission response. Thus, MPF with equivalent negative coefficient has to be realized by tuning the PC2, i.e. $\varphi=0$. The measured transmission response of the MPF is shown in Fig. 2(b). It is a typical high-pass transmission response. The measured result agrees well with the simulated one. We focus on the frequency of 24 GHz which is located at the notch of the transmission response. It should be noted that the notch at 24 GHz is generated by the DIPF rather than the basic transmission response of the MPF. Fig. 2(c) shows the transmission

response of the DIPF. As can be seen, there is a notch at the frequency of 24 GHz. In other words, the notch cannot be changed by adjusting the basic transmission response of the MPF via simply changing the microwave signal driven to the MZM. In the above analysis, the influence of the undesired ± 2-order optical sidebands is not considered. If we take them into account, the simulated result is shown in Fig. 2(d). As can be seen, the contribution of the ± 2-order optical sidebands is very small as they are 11 dB lower than the desired ones, as shown in Fig. 2(a). Actually, the tap number can be extended to five as reported in Ref. [18]. The bias of the MZM and the voltage of the microwave signal driven to the MZM should be 0.32 V_π and 0.59 V_π, respectively.

Next, we tried to let the microwave signal at 24 GHz be located at the peak of the MPF. To do so, the microwave signal driven to the MZM was changed to 12 GHz. The corresponding optical spectrum is shown in Fig. 3(a). At the same time, the PC2 was tuned to let $\varphi = 1.72$ rad. In this way, the DIPF was changed to let the microwave signal at 24 GHz pass. The measured transmission responses of the MPF and the DIPF are shown in Fig. 3(b) and (c), respectively. The simulated result fits well with the measured one. It can be seen that the microwave signal at 24 GHz is located at the peak of the MPF. Thus, the MPF was successfully reconfigured.

Finally, we tried to check the flexibility of the MPF at the other microwave frequency. This time, the microwave signal driven to the MZM was changed to 25 GHz. The optical spectrum is shown in Fig. 4 (a). An out-of-band rejection of 13 dB was observed. The DIPF was again adjusted to produce a high-pass transmission response, i.e. $\varphi = 0$ rad. The transmission responses of the MPF and the DIPF are shown in Fig. 4(b) and (c), respectively. In this case, we focus on the microwave signal at 17 GHz which falls into the notch of the MPF.

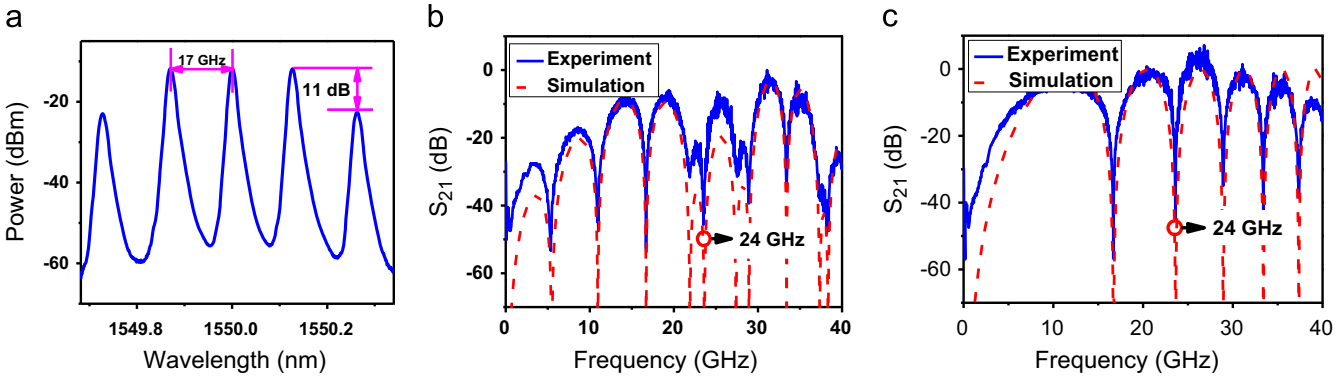

Fig. 2. (a) Measured optical spectrum when the microwave signal driven to the MZM is 17 GHz. Measured and simulated transmission responses of (b) the MPF and (c) the DIPF. Simulated transmission responses of three-tap and five-tap MPFs corresponding to (a).

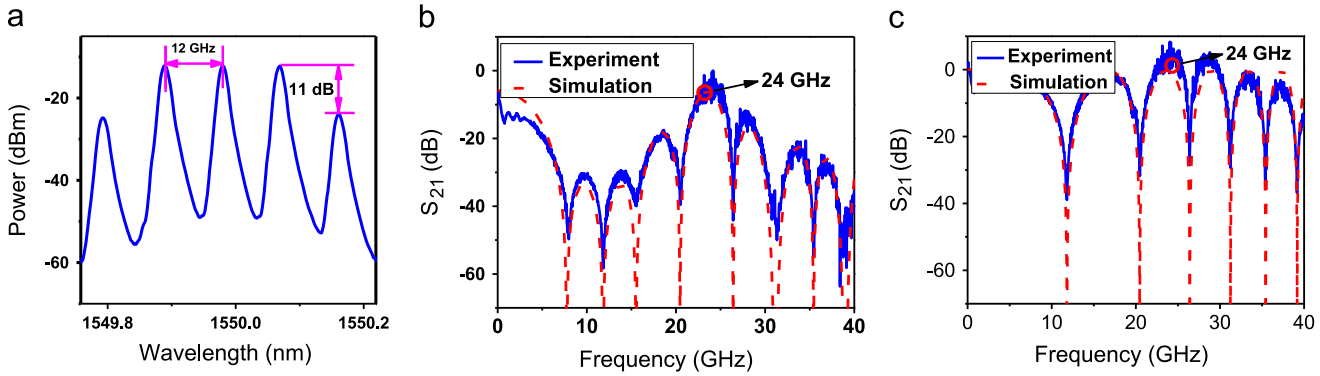

Fig. 3. (a) Measured optical spectrum when the microwave signal driven to the MZM is 12 GHz. Measured and simulated transmission responses of (b) the MPF and (c) the DIPF.

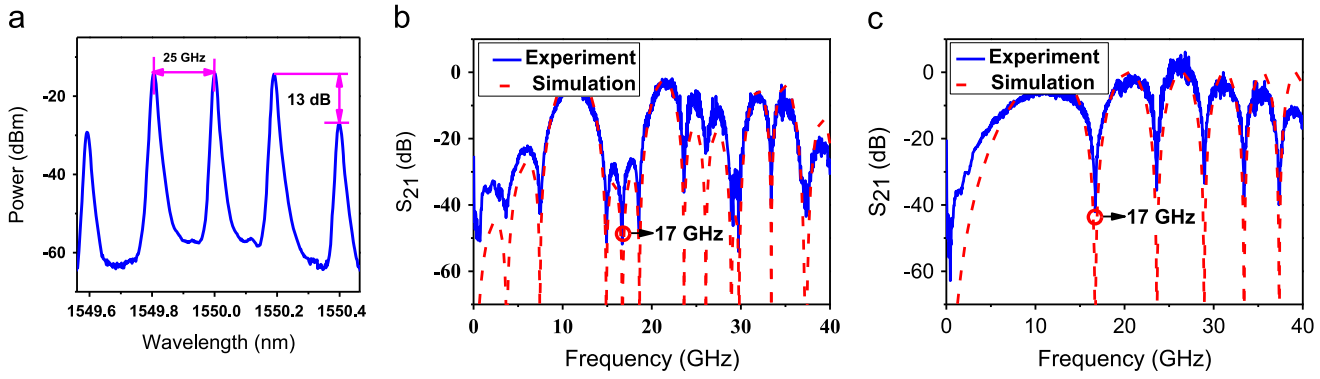

Fig. 4. (a) Measured optical spectrum when the microwave signal driven to the MZM is 25 GHz. Measured and simulated transmission responses of (b) the MPF and (c) the DIPF.

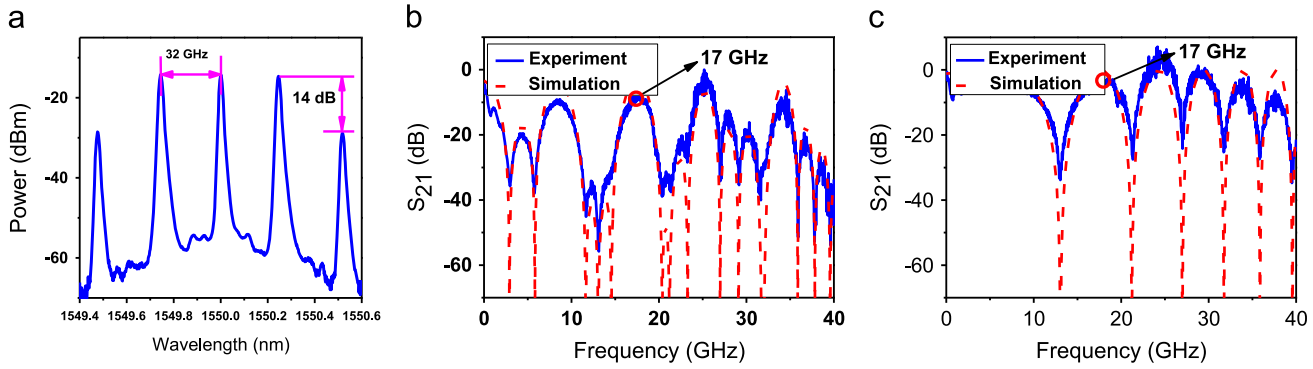

Fig. 5. (a) Measured optical spectrum when the microwave signal driven to the MZM is 32 GHz. Measured and simulated transmission responses of (b) the MPF and (c) the DIPF.

To compensate the loss of the microwave signal at 17 GHz, the MPF was reconfigured by tuning the microwave signal driven to the MZM to 32 GHz and adjusting the PC2 to let $\varphi = 1.22$ rad. The measured optical spectrum is shown in Fig. 5(a), where an out-of-band rejection of 13 dB was achieved. The measured and simulated transmission responses of the MPF as well as the DIPF are shown in Fig. 5(b) and (c), respectively. The MPF was successfully reconfigured to let the microwave signal at 17 GHz pass.

The unflatness of the multi-tap and the poor suppression of the undesired higher-order sidebands will distort the transmission response of the filter. In our experiment, the unflatness of the multi-tap is less than 0.5 dB. Thus, it contributes little to the distortion of the MPF.

In our scheme, the response of the MPF is highly dependent on the SOP of the optical signal. Therefore, two PCs are used in our scheme. For PC1, it is used to align the optical signal with the polarizer integrated in front of the PolM. The variation of the SOP of the optical signal will decrease the optical power, which will finally decrease the gain of the MPF. On the other hand, the PC2 is used to tune the DIPF. So, if the SOP of the optical signal is changed by the environmental disturbance the response of the MPF will be changed. Thus, polarization monitor and feedback control might be required to stabilize the system.

4. Conclusion and discussion

We have demonstrated a reconfigurable MPF based on tunable DIPF in a dispersive element. The multi-tap MPF has been realized using a multi-wavelength optical signal. A polarization modulator (PolM), a polarization controller (PC), and a polarizer are cascaded to build a new modulator which can be regarded as an intensity modulator, a phase modulator, or an intensity and phase hybrid modulator by adjusting the PC. A dispersive fiber is followed after the PC to generate the DIPF. The key significance of the proposed MPF is that, the DIPF is tunable by adjusting the PC. In this way, not only low-pass but also high-pass MPFs can be achieved. The proposed scheme has been theoretically analyzed and experimentally verified. The experimental results show that the proposed MPF is highly reconfigurable and tunable.

It should be noted that the PolM used in our scheme cannot be replaced by a MZM which can also generate double-sideband (DSB) modulated signal. For the MZM, the phase difference between the optical carrier and sidebands is fixed. However, the phase difference between the optical carrier and sideband are arbitrarily tunable for a PolM, which results in a tunable DIPF as well as a tunable MPF.

Acknowledgments

This work was supported by the National Natural Science Foundation of China under 61377069, 61335005, 61108002, 61321063, and 61090391.

References

[1] R.A. Minasian, IEEE Trans. Microw. Theory Tech. 54 (2) (2006) 832.
[2] J. Capmany, B. Ortega, D. Pastor, J. Lightw. Technol. 24 (1) (2006) 201.
[3] J. Capmany, J. Mora, I. Gasulla, J. Sancho, J. Lloret, S. Sales, J. Lightw. Technol. 31 (4) (2013) 571.
[4] J.P. Yao, J. Lightw. Technol. 27 (3) (2009) 314.
[5] J. Capmany, D. Pastor, A. Martinez, B. Ortega, S. Sales, Opt. Lett. 28 (16) (2003) 1415.
[6] J. Li, K. Xu, J. Wu, J. Lin, Opt. Commun. 282 (5) (2009) 845.
[7] C.K. Oh, T.Y. Kim, S.H. Baek, C.S. Park, Opt. Express 14 (15) (2006) 6628.
[8] E.M. Xu, X.L. Zhang, L. Zhou, Y. Zhang, Y. Yu, X. Li, D.X. Huang, Opt. Lett. 35 (8) (2010) 1242.
[9] E.H.W. Chan, R.A. Minasian, IEEE Trans. Microw. Theory Tech. 58 (11) (2010) 3199.
[10] K. Zhu, H. Ou, C. Ye, H. Fu, S. He, Opt. Commun. 284 (1) (2011) 140.
[11] F. Zeng, J. Yao, Opt. Express 12 (16) (2004) 3814.
[12] F. Zeng, J.P. Yao, J. Capmany, J. Lightw. Technol. 23 (4) (2005) 1721.
[13] H.Y. Ou, K. Zhu, C.H. Ye, Y. Hu, IEEE Photonics Technol. Lett. 23 (14) (2011) 938.
[14] X.X. Xue, X.P. Zheng, H.Y. Zhang, B.K. Zhou, J. Lightw. Technol. 31 (13) (2013) 2263.
[15] W. Li, L.X. Wang, M. Li, N.H. Zhu, Opt. Lett. 38 (17) (2013) 3441.
[16] H.T. Zhang, S.L. Pan, M.H. Huang, X.F. Chen, Opt. Lett. 36 (5) (2012) 866.
[17] Z.Z. Tang, S.L. Pan, D. Zhu, R.H. Guo, Y.J. Zhao, M.H. Pan, D. Ben, J.P. Yao, IEEE Photonics Technol. Lett. 5 (2) (2012) 1487.
[18] W.H. Sun, W. Li, W.T. Wang, J.G. Liu, N.H. Zhu, Opt. Commun. 321 (2014) 73.